第 30 卷第 2 期
2014 年 2 月

无 机 化 学 学 报
CHINESE JOURNAL OF INORGANIC CHEMISTRY

Vol.30 No.2
451-458

二氧化锡薄膜:制备及在室温下气敏性质

郝沛沛[1] 陈长龙*,[1] 魏玉玲[2] 穆晓慧[1]
([1]济南大学化学化工学院,济南 250022)
([2]齐鲁工业大学分析测试中心,济南 250353)

摘要:利用溶胶–凝胶法首先在玻璃基片上制备了氧化锡晶种膜,之后采用溶剂热法在其上生长了致密的氧化锡薄膜。利用扫描电子显微镜和 X 射线衍射技术对氧化锡薄膜的形貌和晶体结构进行了表征,结果表明构成薄膜的氧化锡晶粒具有四方锡石结构,尺寸在 7~10 nm 之间。表面活性剂在溶剂热反应过程中对薄膜生长的研究表明,十二烷基苯磺酸钠可以显著提高薄膜的质量。对所制备的氧化锡薄膜进了气敏性质研究,结果表明,在温和的测试条件下,如室温、常压、干燥的空气背景等,该氧化锡薄膜对二氧化氮气体具有良好的探测能力,检测限为 0.5 μL·L^{-1}。

关键词:薄膜;X–射线衍射;半导体;气体传感器
中图分类号:O611.4 **文献标识码**:A **文章编号**:1001-4861(2014)02-0451-08
DOI:10.11862/CJIC.2014.046

Tin Oxide Thin Films: Synthesis and Room Temperature Gas Sensing Properties

HAO Pei-Pei[1] CHEN Chang-Long*,[1] WEI Yu-Ling[2] MU Xiao-Hui[1]
([1]*School of Chemistry and Chemical Engineering, University of Jinan, Jinan* 250022, *China*)
([2]*Instrumental Analysis Center, Qilu University of Technology, Jinan* 250353, *China*)

Abstract: Dense tin oxide films were solvothermally grown from the tin oxide seed films fabricated on glass substrates by sol-gel technique. The morphology and crystal structure of the tin oxide films were characterized by using scanning electron microscopy and X-ray diffraction techniques. The results reveal that the films are composed of cassiterite-type tin oxide crystals with size of 7~10 nm. The film quality can be improved significantly when the sodium dodecylbenzenesulfonate is used as the surfactant during the solvothermal reaction. The gas sensor, which is directly connected tin oxide films to the test circuits by using tweezers with special gripping surfaces, exhibits good sensing performance to nitrogen dioxide gas under mild testing conditions, i.e. room temperature, ambient pressure, and dry air background. The sensor can achieve a detection limit of 0.5 μL·L^{-1}.

Key words: thin films; X-ray diffraction; semiconductors; gas sensor

0 Introduction

In recent years, oxide semiconductor nanomaterials have attracted much attention due to their novel properties and potential applications [1-3]. Tin dioxide (SnO_2), an n-type semiconductor material, is widely used in many fields such as solar cells, catalysts, electrodes and gas sensors owing to its potential applications [4-7]. The nanostructured SnO_2 exhibits high electrical conductivity and high optical

收稿日期:2013-07-19。收修改稿日期:2013-10-15。
国家自然科学基金(No.20901029)资助项目。
*通讯联系人。E-mail:chm_chencl@ujn.edu.cn, Tel: +86-531-82765475

transparency in the visible part of the spectrum, and is regarded as one type of the important future semiconductor materials that can be used to enhance the properties of the sensors [8-9]. Compared with other SnO_2 nanostructures, the SnO_2 thin films could exhibit greatly enhanced gas sensing performance due to the small grains and large specific surface area [10]. Accordingly, preparing SnO_2 thin films on special substrates is an effective strategy to obtain high performance gas sensors. A lot of methods including sputtering [11-12], chemical vapor deposition (CVD)[13], pulsed laser deposition (PLD) [14], and sol-gel processing [15] have been developed for preparation of SnO_2 thin films. In these methods, the sol-gel technique is particularly attractive due to its low cost, simplicity and applicability for large-scale production [16-17]. However, SnO_2 thin films fabricated by sol-gel technique sometimes have the shortcomings as instability and poor smoothness [18]. Thus, exploring simple and effective synthetic method to achieve high quality SnO_2 thin film is still quite challenging.

As one of the several properties, the gas sensing performance of SnO_2 attracts much attention due to the increasingly serious environmental problems. Quickly and selectively detecting the target gas is the ability that an excellent sensor should possess. Recently many attempts such as doping and modification have been made to improve the gas sensing ability of the SnO_2-based sensors. For example, S.P. Gong et al [19] reported that the sensing performance of the SnO_2 thin film sensors could be enhanced by adopting the Cu-doping. Rajpure et al[20] also reported the improvement of gas sensing ability of the SnO_2 film sensors via doping with 1% Sb. In addition, the measurement temperature is also an important factor much considered in the gas sensing tests. For example, Mishra et al[16] observed that the peak value of the gas sensing sensitivity of the SnO_2 film sensors occurred at around 623 K. Rella et al [17] achieved the promoted gas sensing ability of the SnO_2 thin film sensors by setting the measurement temperature at above 200 ℃. However, gas sensing measurements conducted at high temperature are much complex in comparison with those conducted at room temperature. Therefore, if a gas sensor can effectively detect a target gas at temperature as close as possible to the room temperature, it will be more suitable for the real world applications.

In this paper, we report the solvothermal growth of dense SnO_2 thin films from the SnO_2 seed films fabricated on glass substrates by sol-gel technique. Without further complicated electrical contact work, we directly connect the small cut pieces, i.e., the small pieces of SnO_2 thin film together with the glass substrate, to the test circuits and measure their gas sensing behavior. It reveals that the SnO_2 thin films obtained by the two-step method are smooth, dense and continuous. When used as gas sensors, the SnO_2 thin films exhibit good sensing performance to nitrogen dioxide (NO_2) gas.

1 Experimental

1.1 Materials

Tin (Ⅳ) chloride pentahydrate ($SnCl_4 \cdot 5H_2O$) and cetyltrimethyl ammonium bromide (CTAB) were purchased from Sinopharm Chemical Reagent Co., Ltd. Tin (Ⅱ) chloride dehydrate ($SnCl_2 \cdot 2H_2O$) and sodium dodecyl sulphate (SDS) were purchased from Guangcheng Chemical Reagent Plant, Tianjin. Anhydrous ethanol, sodium hydroxide (NaOH), and sodium dodecylbenzenesulfonate (SDBS) were purchased from Damao Chemical Reagent Plant, Tianjin. All materials were used without further purification.

1.2 Preparation of SnO_2 seed films

The SnO_2 seed films were fabricated through the sol-gel method. In a typical synthesis, $SnCl_2 \cdot 2H_2O$ (6.770 g) was dissolved in anhydrous ethanol (40 mL), and then the solution was transferred into a round-bottomed flask for circumfluence at 82 ℃ for 10 h. After aging for 64 h at room temperature, the weak yellow sol was obtained. Before preparing the gel films, the glass substrates (76.2 mm×25.4 mm×1.0 mm, Xintai Medical Equipment Factory, Yancheng, China.) were cleaned sufficiently by ultrasonication in deionized water and ethanol, respectively. The gel

films on glass substrates were fabricated by dip-coating technique, in which the dropping rate was set at 9 cm·min^{-1}, and then the films were dried at 200 ℃ for 15 min. The above cycle was repeated five times and the obtained gel films were annealed at 600 ℃ for 1 h to form the oxide films, which were then cut into small pieces with dimensions of 25.4 mm×10.0 mm×1.0 mm and were used as seed films in the following solvothermal growth.

1.3 Solvothermal growth of SnO_2 thin films from the SnO_2 seed films

In a typical procedure, 15 mL of ethanol solution containing 0.320 g $SnCl_4·5H_2O$ and 0.1 g SDBS as surfactant was poured into a 20 mL Teflon lined autoclave, and then 0.04 g NaOH was added. The small SnO_2 seed film on glass substrate was immersed into the solution and kept against the wall of the autoclave. After being heated at 180 ℃ for 6 h, the autoclaves were cooled to room temperature. The resulting samples were taken out and washed with deionized water to remove the impurity ions. After air drying, the SnO_2 dense films were obtained.

1.4 Characterization

X-ray diffraction (XRD) patterns of the samples were recorded in the range of 2θ=15°~75° on an X-ray diffractometer (Bruker D8 Advance) with a LynxEye detector using Cu $K\alpha$1 radiation (λ = 0.154 06 nm) at room temperature while the voltage and electric current were held at 40 kV and 30 mA, respectively. The morphologies of the products were determined by scanning electron microscopy (SEM, FEI Quanta FEG 250) with the voltage of 10.00 kV. During the SEM measurements, a small piece of sample was adhered onto a copper stub using double-sided carbon tape. Fourier transform infrared (FTIR) spectra were recorded using a Shimadzu IRPrestige-21 Fourier transform infrared spectrometer using the KBr pellet technique in the range of 400~4 000 cm^{-1}.

1.5 Sensor Fabrication and Tests

After heat treating at 200 ℃ for 6 h, the SnO_2 thin film was directly connected to the test circuit by using tweezers with special gripping surfaces and put into the airtight test chamber with capacity of 300 mL to conduct the gas sensing tests. During the tests, clean dry air flow and static NO_2/air mixed gas were introduced into the chamber alternately. The electric current of the sensors was recorded using a HP 4140B pA Meter/DC voltage source.

2 Results and discussion

2.1 Morphology and Structure

Fig.1a shows the SEM image of the SnO_2 thin film synthesized with adding 0.1 g of SDBS to the autoclave. As can be seen, the film is quite flat and smooth without obvious cracks. The cross-sectional image of the film shown in the inset reveals that the film is composed of small nanocrystals and has a thickness of ~490 nm. No obvious cracks or large pores are found on the cross-section, which further confirms its continuity. When observing at higher magnification (shown in Fig.1b), uniform small grains can be clearly distinguished, further confirming the smoothness of the film. The effect of other surfactants on the SnO_2 films quality was also investigated. Using 0.1 g of SDS as surfactant, as can be seen from Fig. 1c, the solvothermally grown SnO_2 film shows wide and cross-linked cracks, displaying poor continuity. When 0.1 g of CTAB was used in the solvothermally growth, the prepared film is full of hollows although it is not cracked (Fig.1d). It indicates that different surfactants can significantly affect the quality of the formed films. In order to make a comparison, we also prepared SnO_2 films without using any surfactants. As seen from Fig.1e, the film obtained without using surfactant also shows cracks, but they are much thinner than those of the film shown in Fig.1c. At the same time, the film shows poorer smoothness. There are scattered spherical particles occurred on the film surface. The cracking phenomenon is ascribed to the large surface tension of the films, which might occur during or after the solvothermal process. Fig.1f shows the SEM image of the seed film. As shown, the seed film has no obvious cracks but the composed particles are arranged loosely. It may result from the limited dip-coating cycles during the sol-gel process. When the dip-coating procedure during the sol-gel process is

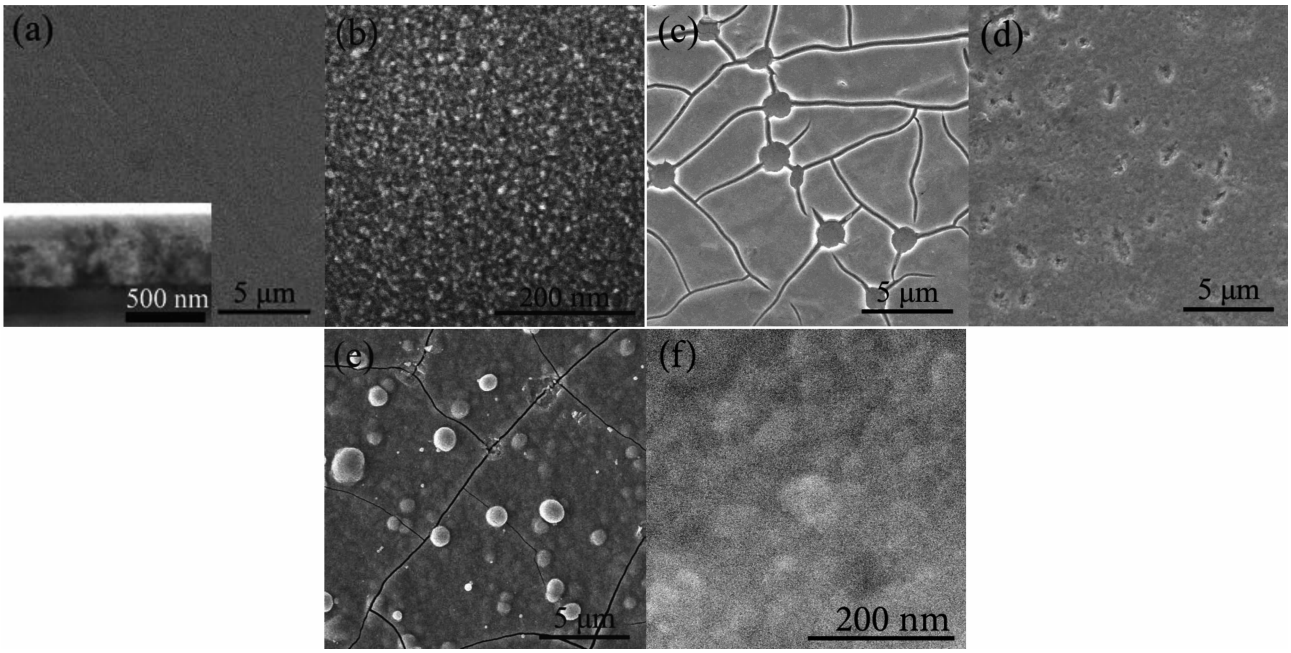

Fig.1 SEM images of SnO_2 thin films prepared solvothermally at 180 ℃ for 6 h with (a, b) 0.1 g SDBS, (c) 0.1 g SDS, (d) 0.1 g CTAB, and (e) without surfactant. (f) SEM image of SnO_2 seed film. The inset is the cross-section image of SnO_2 films prepared with 0.1 g SDBS

repeated for more than 5 times, however, cracks will appear on the formed seed films (not shown).

Fig.2 shows three XRD patterns, i.e., pattern a, b, and c, which originate from the seed film, the solvothermally grown SnO_2 film with 0.1 g of SDBS as surfactant (denoted as SDBS-film), and the solvothermally grown SnO_2 film without using surfactant (denoted as surfactant-free-film), respectively. As can be seen, the three samples show similar diffractions, indicating that they are composed of the same crystal structure grains. According to the diffraction characteristics, the crystal phase can be ascribed to the cassiterite-type SnO_2 (PDF No. 41-1445). The crystal sizes estimated by applying the Scherrers equation to the line broadening of the (101) peaks of pattern a, b, and c are 7.5, 7.9, and 8.4 nm, respectively.

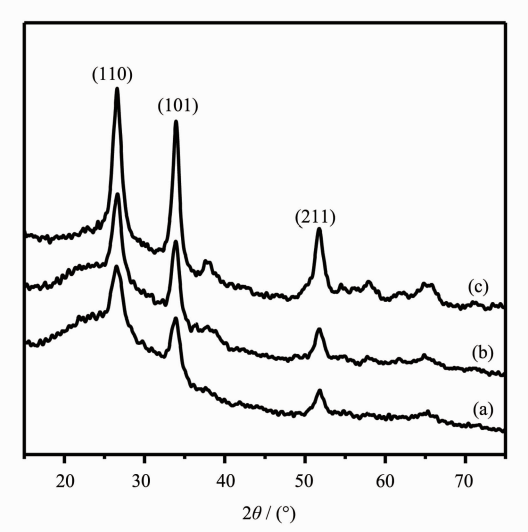

Fig.2 XRD patterns of (a) SnO_2 seed film, (b) solvothermally grown SnO_2 film with 0.1 g SDBS (SDBS-film), and (c) solvothermally grown SnO_2 film without surfactant (surfactant-free-film)

In addition, as shown, the diffraction intensity of these three films, i.e., the seed film, the SDBS-film, and the surfactant-free-film, increases orderly. In this work, the seed films were prepared by sol-gel technique, in which five dip-coating cycles followed an annealing treatment were conducted. Thus the obtained seed films are very thin and would result in weak XRD intensity (Fig.2a). With new SnO_2 grains grown on the seed film, the film thickness increases and therefore patterns b and c show stronger XRD intensity than that of pattern a. During the solvothermal process, it can be speculated that the seed film induces the heterogeneous nucleation of the

new SnO_2 nuclei, which further grow to form thicker film. To verify this speculation, additional solvothermal growth experiments were conducted by using naked glass substrates substituting for the seed films while the other reaction conditions were kept constant. It is found that SnO_2 could not grow on the naked glass substrates no matter whether the surfactant is used or not. It suggests that the seed film is necessary for the solvothermal growth of new SnO_2 grains. In addition, the XRD intensity of the surfactant-free-film is a little stronger than that of SDBS-film. It is sure that the introduction of the surfactant does affect the SnO_2 nucleation and growth. But the true effect of the surfactants on the solvothermal growth of SnO_2 film needs further investigation. We speculate that the SDBS molecules may be adsorbed on some special crystal planes of SnO_2 during the solvothermal preparation and thus vary the surface energy, which in turn affects the SnO_2 nucleation and growth. There are many similar preparations using surfactant molecules to affect the crystal nucleation and growth[21-22].

2.2 Gas-sensing performance of the SnO_2 thin films

We use the solvothermally grown SnO_2 thin films as gas sensors to detect NO_2 gas. Because the quality of the films prepared using SDS and CTAB as surfactants are low, the gas sensing tests are focused on the SnO_2 film prepared with SDBS as the surfactant and the surfactant-free SnO_2 film. The gas sensing tests were operated in a homemade apparatus with chamber capacity of 300 mL, which is schematically shown in Fig.3. Nitrogen dioxide (NO_2) molecules as electron-withdrawing species can be adsorbed on the SnO_2 thin film, which will result in the electron

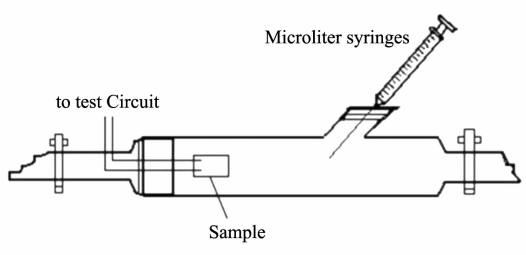

Fig.3　Schematic diagram of the gas-sensing test apparatus

density decrease of the film and thus lead to the decrease of the conductance. As the conductance of the wide bandgap SnO_2 itself is low, a 20 V dc bias is held between the two tweezers during the tests. To make the tests as close as possible to the real-world application of gas sensors, all gas sensing tests were carried out at mild conditions, i.e., room temperature, ambient pressure, dry air background.

During the tests, every exposure of the sensor to the static NO_2/dry air mixed gas is separated by an exposure to dry air flow. The sensor sensitivity (S) is defined in Equation(1)[23]:

$$S = \frac{R_{gas}}{R_{air}} = \frac{U/I_{gas}}{U/I_{air}} = \frac{I_{air}}{I_{gas}} \quad (1)$$

where R is the resistance of the sensors, I is the electric current that flows through the sensors when a constant dc bias U is held between the two tweezers. The subscripts "air" and "gas" designate the two parameters R and I in air and in target gas, respectively. Before the gas-sensing tests, the SnO_2 thin films are heat treated at 200 ℃ for 6 h to make the sensors be stable.

Fig.4a shows the typical room temperature dynamic response/recovery curve of the SnO_2 SDBS-film sensor. It shows that the sensor is very sensitive to the variation of the NO_2 gas concentration. When NO_2 gas concentrations are adjusted to 0.5, 1.0, 5.0, 10, and 50 $\mu L \cdot L^{-1}$, the signals (areas) given by the sensor are about 3, 8, 82, 200, and 365, respectively. Table 1 lists the raw data of the noise and signal of the sensor exposed to 0.5, 1.0 and 5.0 $\mu L \cdot L^{-1}$ NO_2 gases. As seeing, when the NO_2 concentration increases to 0.5 $\mu L \cdot L^{-1}$ the sensor gives a signal-to-noise ratio of ~3. According to the method used to determine the detection limit and the quantification limit, i.e., they are three times and ten times of the signal-to-noise ratio, respectively, the detection limit and quantification limit for our sensor are estimated to be 0.5 and 1.3 $\mu L \cdot L^{-1}$, respectively. In addition, the sensor also exhibits room-temperature fast response/recovery ability. In our experiments, the response and recovery times are set at 400 s and 600 s, respectively. As shown, such a cycle time is enough

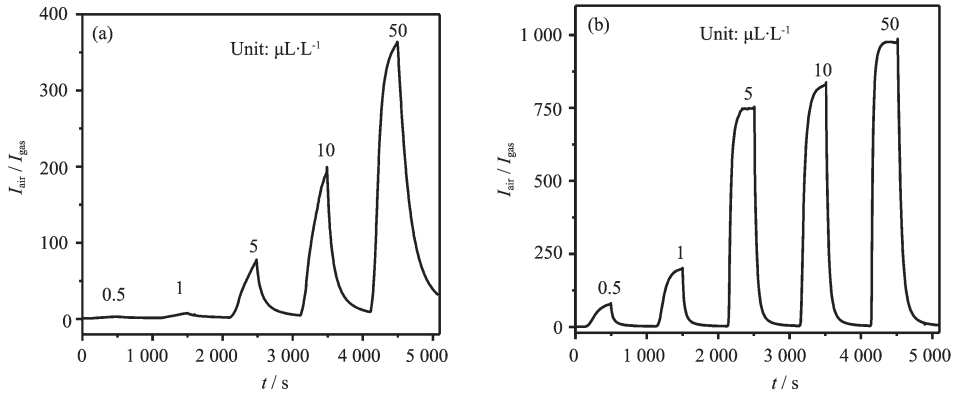

Fig.4 Room temperature gas-sensing response/recovery curves of (a) SnO_2 SDBS-film and (b) SnO_2 surfactant-free-film sensors

Table 1 Raw data of the gas sensing of SnO_2 SDBS-film to 0.5, 1.0 and 5.0 $\mu L \cdot L^{-1}$ NO_2 gases

NO_2 concentration / ($\mu L \cdot L^{-1}$)	0.5	1	5
Noise / $Area^{-1}$		4.46×10^5	
Signal / $Area^{-1}$	1.41×10^6	3.45×10^6	3.46×10^7
Signal to Noise ratio	3	8	78

for the sensor to distinguish the different concentrations of the target gases, which is much shorter than many reported results [24-25].

Fig.4b shows the response/recovery curve of the SnO_2 surfactant-free-film sensor. As seen, this film sensor is also very sensitive to NO_2 gas. Compared with the SDBS-film sensor, the surfactant-free-film sensor even shows higher gas sensing ability. For instance, when exposed to 5 $\mu L \cdot L^{-1}$ of NO_2 gas, the surfactant-free-film sensor and the SDBS-film sensor give S values of 751 and 78, respectively. It is presumably that the SnO_2 crystals of the surfactant-free-film have clean surfaces due to the surfactant-free synthetic process such that they possess higher activity in NO_2 molecule absorbing than the SnO_2 crystals of the SDBS-film do when exposed to a certain concentration of NO_2 gas[26]. For the SDBS-film, the residual surfactant molecules on crystals may interfere with the thorough interaction between the crystals and the target gas, and thus its sensitivities would be weakened a little bit. To confirm the existence of the residual surfactant molecules on the SnO_2 SDBS-film, the film was scraped from the glass substrates and analyzed by using IR spectrum. For comparison, the IR spectrum of the SnO_2 surfactant-free-film was also measured. As shown in Fig.5a, the both spectra reveal the Sn-O vibrations at around 660 cm^{-1} [27] and the O-H vibrations at about 3 350 and 1 627 cm^{-1}[28]. For SnO_2 SDBS-film, however, there are some weak vibrations in the range of 1 000~1 200 cm^{-1}, which can be ascribed to the sulfonate stretching vibrations[29]. Although the shown sulfonate stretching vibrations are very weak, they still confirm the existence of the residual surfactant molecules on the SnO_2 SDBS-film. On the other hand, we have tried to remove the residual surfactant molecules on the SnO_2 SDBS-film but have found from the IR spectrum (not shown) that the surfactant still exists even the sample after being rinsed with a large quantity of water for 6 h. Extending the washing time more than 10 h, the SnO_2 film would be ruined and would detach from the glass substrate. An alternative reason for the higher sensitivity of the SnO_2 surfactant-free-film sensor than that of the SDBS-film sensor may be the higher surface to volume ratio of the former. As shown in Fig. 6, the surface of the surfactant-free-film is quite rough, which may provide more active sites for the gas-sensing than the relatively flat SDBS-film does.

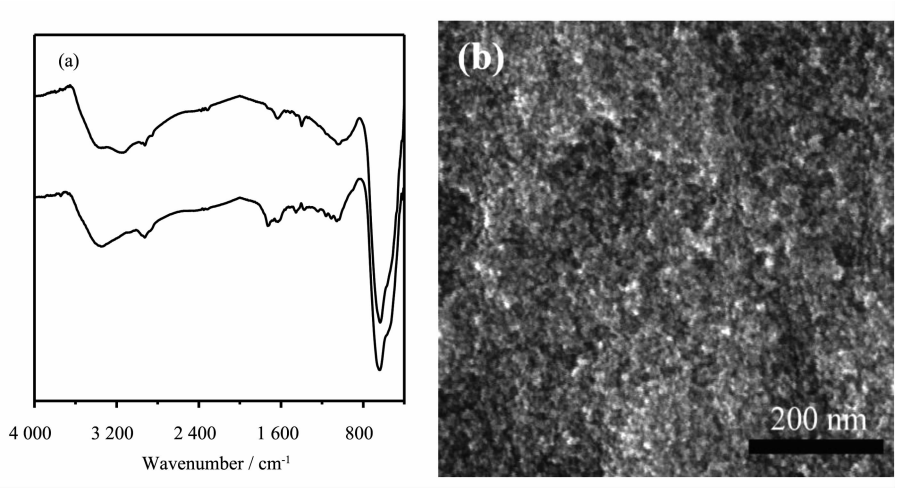

Fig.5　(a) FTIR spectra of SnO_2 surfactant-free-film (top) andSnO_2 SDBS-film (botttom); (b) High magnification SEM image of SnO_2 surfactant-free-film

On the whole, however, the surfactant-free-film sensor shows lower discrimination ability to the different concentrations of target gases than the SDBS-film sensor does, especially when the NO_2 gas concentration is higher than 5 $\mu L \cdot L^{-1}$ (Fig.4b). It may be due to the fast response ability of the surfactant-free-film sensor. In other words, once the target gas concentration is higher than 5 $\mu L \cdot L^{-1}$, the sensor is easy to get to saturated adsorption, and thus it shows much weaker discrimination ability to higher concentrations of target gases.

Fig.6 illustrates the sensing behavior of the SnO_2 SDBS-film sensor towards 5 $\mu L \cdot L^{-1}$ of NO_2 and 5 $\mu L \cdot L^{-1}$ of carbon monoxide (CO) gases. As can be seen, in comparison with the first three responses of the sensor to 5 $\mu L \cdot L^{-1}$ of NO_2, the response of the sensor to 5 $\mu L \cdot L^{-1}$ CO gas is much weaker. It is so weak that it is hard to confirm whether the signal does come from the sensing response to the gas sample or just is the disturbance effect of the test system caused by the sample injection. After the cycle of 5 $\mu L \cdot L^{-1}$ CO sample, the followed injection of 5 $\mu L \cdot L^{-1}$ NO_2 sample makes the sensor again give normal response/recovery. Keeping the test procedure constant, tests conducted using the SnO_2 surfactant-free-film as sensor give similar results. It indicates that the film sensor can hardly sensitive to the 5 $\mu L \cdot L^{-1}$ CO gas.

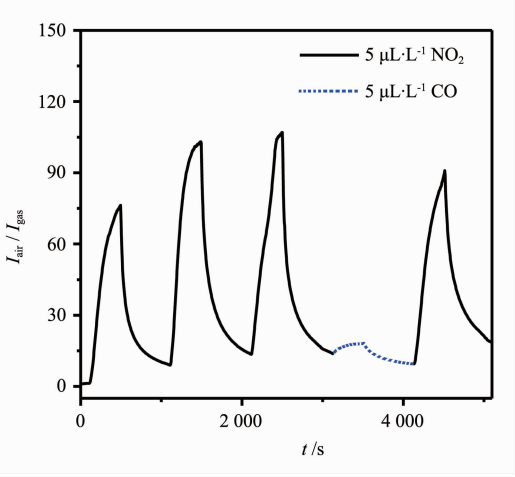

Fig.6　Room-temperature gas-sensing response/recovery curve of the SnO_2 SDBS-film towards 5 $\mu L \cdot L^{-1}$ of NO_2 gas and 5 $\mu L \cdot L^{-1}$ of CO gas

3　Conclusions

In summary, high quality of SnO_2 thin films on glass substrates were prepared solvothermally from the seed films fabricated by sol-gel technique. The synthetic procedure has the merit of simplicity and low cost. It reveals that using SDBS as the surfactant can significantly improve the film quality during the solvothermal reaction. When used as gas sensors, the SnO_2 SDBS-films show good gas sensing performance to NO_2 gas at mild test conditions such as room temperature, ambient pressure, and dry air background, and a detection limit of about 0.5 $\mu L \cdot L^{-1}$ is achieved. The surfactant-free-films show a little bit

inferior discrimination ability to different concentrations of NO_2 gases although their responses to sample gases are quite high, which is ascribed to their easiness of reaching the saturated adsorption due to the SnO_2 crystals clean surfaces as well as its higher surface to volume ratio. The SnO_2 films also exhibit good sensing selectivity. When exposed to 5 $\mu L \cdot L^{-1}$ of CO gas, the sensors show no obvious responses.

Acknowledgments: This work was supported by the National Natural Science Foundation of China (No. 20901029) and the Promotive Research Fund for Excellent Young and Middle-aged Scientists of Shandong Province (No. BS2009CL018).

References:

[1] Vomiero A, Bianchi S, Comini E, et al. *Cryst. Growth Des*., **2007**,**7**:2500-2504

[2] Ghimbeu C M, Lumbreras M, Siadat M, et al. *Mat. Sci. Semicon. Proc*., **2010**,**13**:1-8

[3] Tamiolakis I, Lykakis I N, Katsoulidis A P, et al. *Chem. Mater.*, **2011**,**23**:4204-4211

[4] Kim Y J, Kim K H, Kang P, et al. *Langmuir*., **2012**,**28**: 10620-10626

[5] Gavagnin R, Biasetto L, Pinna F, et al. *Appl. Catal. B*: *Environ*., **2002**,**38**:91-99

[6] Zhu J J, Lu Z H, Aruna S T, et al. *Chem. Mater*., **2000**,**12**: 2557-2566

[7] Gardeshzadeh A R, Raissi B. *Mat. Sci. Semicon. Proc*., **2010**, **13**:151-155

[8] Gong J W, Chen Q F, Fei W F, et al. *Sens. Actuators B.*, **2004**,**102**:117-125.

[9] Ding J J, Yan X B, Li J, et al. *ACS. Appl. Mater. Interfaces*, **2011**,**3**:4299-4305

[10]Fang Y K, Lee J J. *Thin Solid Films*, **1989**,**169**:51-56

[11]Chacko S, Philip N S, Gopchandran K G, et al. *Appl. Surf. Sci.*, **2008**,**254**:2179-2186

[12]Ghosh S, Khan G G, Mandal K. *ACS Appl. Mater. Interfaces*, **2012**,**4**:2048-2056

[13]Pan J, Song X F, Zhang J, et al. *J. Phys. Chem. C*, **2011**, **115**:22225-22231

[14]Chen Z W, Pan D Y, Zhao B, et al. *ACS Nano*., **2010**,**4**: 1202-1208

[15]da Silva V D L, de Andrade A, Scalvi L V A, et al. *Mater. Chem. Phys*., **2012**,**134**:994-1000

[16]Mishra S, Ghanshyam C, Ram N, et al. *Bull. Mater. Sci.*, **2002**,**25**:231-234

[17]Rella R, Serra A, Siciliano P, et al. *Sens. Actuators B*, **1997**, **44**:462-467

[18]Acciarri M, Canevali C, Mari C M, et al. *Chem. Mater*., **2003**,**15**:2646-2650

[19]Gong S P, Xia J, Liu J Q, et al. *Sens. Actuators B*, **2008**, **134**:57-61

[20]Rajpure K Y, Kusumade M N, Neumann-Spallart M N, et al. *Mater. Chem. Phys*., **2000**,**64**:184-188

[21]Ramos L, Lubensky T C, Dan N, et al. *Science*, **1999**,**286**: 2325-2328

[22]Jang J H, Park J H, Oh S G. *J. Ceram. Process. Res*., **2009**, **10**:783-790

[23]Chen C L, Wei Y L, Sun G X, et al. *Chem. Asian J*., **2012**, **7**:1018-1025

[24]Gyger F, Hübner M, Feldmann C, et al. *Chem. Mater.*, **2010**,**22**:4821-4827

[25]DArienzo M, Armelao L, Cacciamani A, et al. *Chem. Mater*., **2010**,**22**:4083-4089

[26]Chen C L, Wei Y L, Chen D R, et al. *Mater. Chem. Phys*., **2011**,**125**:299-304

[27]Tocchetto A, Glisenti A. *Langmuir*., **2000**,**16**:2642-2650

[28]Sun C T, Xue D F. *J. Phys. Chem C.*, **2013**,**117**:19146-19153

[29]Michiya M, Serizawa, Kishida A, et al. *Bioconjugate Chem.*, **2002**,**13**:23-28